Experimental and 3D numerical analysis on the effect of specimen thickness on fracture toughness of Al6061-SiC-cenosphere hybrid composites

E. Ashoka
Department of Mechanical Engineering, Bapuji Institute of Engineering and Technology, Davangere, India.
ashokamech06@gmail.com; http://orcid.org/0000-0002-3062-5883

T. H. Manjunatha*
Department of Mechanical Engineering, Ballari Institute of Technology and Management, Ballari-583104, Karnataka India.
manjuforeverthree@gmail.com; http://orcid.org/0000-0002-2794-797X

H. S. Naveen Kumar
Department of Mechanical Engineering, Government Polytechnic, Holenarasipura–573211, Karnataka, India.
naveen.2416932@ka.gov.in; http://orcid.org/0000-0001-8203-3460

S. V. Lingaraju
Department of Mechanical Engineering, Tatyasaheb Kore Institute of Engineering and Technology Warananagar, Warana University, Kolhapur, India
svlingaraju@tkietwarana.ac.in; http://orcid.org/0000-0003-3882-8228

H. N. Ravikumar
Department of Mechanical Engineering, Bapuji Institute of Engineering and Technology, Davangere, India.
ravikumarhn85@gmail.com; https://orcid.org/0009-0000-4327-9134

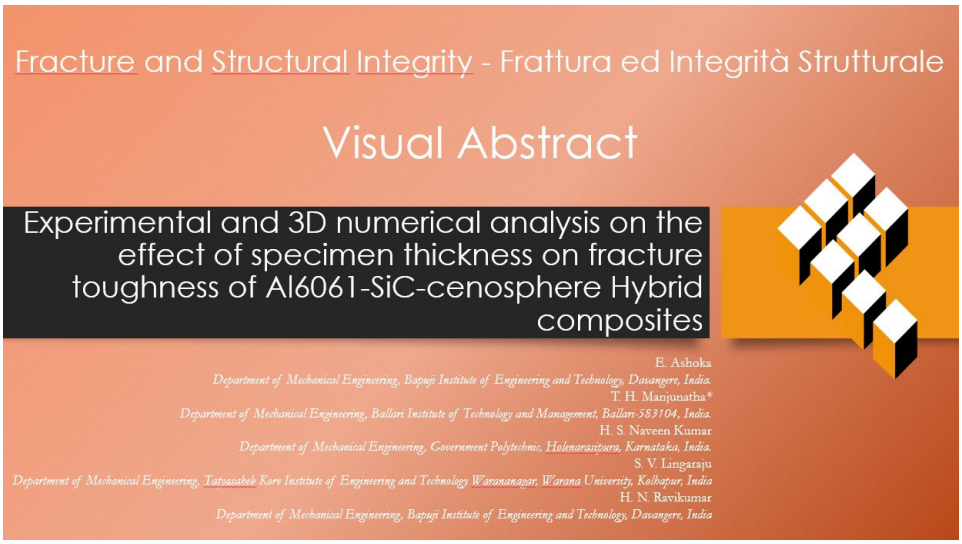

Citation: Ashoka, E., Manjunatha, T. H., Naveen Kumar, H. S., Lingaraju, S. V., Ravikumar, H. N. Experimental and 3D numerical analysis on the effect of specimen thickness on fracture toughness of Al6061-SiC-cenosphere hybrid composites, Fracture and Structural Integrity, 75 (2026) 265-280.

Received: 15.09.2025
Accepted: 29.10.2025
Published: 05.11.2025
Issue: 01.2026

KEYWORDS. Al6061 alloy, a/W, B/W ratios, Fracture toughness, Cenosphere, CT specimens.

INTRODUCTION

Aluminium alloys are applied widely for engineering purposes because of their high strength-to-weight ratio, ease of machining, and resistance against corrosion. Among them, aluminum alloy (Al6061) is of interest because of its homogeneity in mechanical properties like toughness, strength, and weldability. They find best application in structural use in the aerospace, automobile, and marine fields [1]. Al6061 alloy has magnesium and silicon as its major alloying elements that strengthen its hardness, strength and corrosion resistance when it is still lightweight in nature [2]. Still, to prolong its mechanical properties even under severe loading conditions, Al6061 is normally hybridized with other materials to produce hybrid composites [3].

Hybrid Al6061 matrix composites consist of Al6061 reinforcement phases such as silicon carbide (SiC) particles and cenospheres. SiC particles (SiCp) are more hard, thermally stable and provide wear resistance immensely improving the stiffness and load carrying capacity of the aluminum [4]. Cenospheres are actually hollow ceramic microspheres with weight saving and better insulation properties. The combination of cenosphere particles with SiC creates a new material offering the best combination of light weight, stiffness, and strength. In automobile and aerospace industries, such aluminium matrix composites (AMCs) are already being used where high strength was coupled with lesser weight. Yet, knowing about the fracture behavior of AMCs, especially their cracking sensitivity to initiation as well as propagation, is vital to guaranteeing their reliability to structural applications [5,6].

Fracture toughness is one of the material's established properties that represents the material's ability to withstand crack growth and is critical to determining failure when under loading with crack-like defects. Fracture toughness is characterized by a compact tension (CT) test, a standard test for measuring stress intensity factor (SIF) at a crack location [7]. Fracture toughness (FT) tests give information regarding a material's capability for crack growth tolerance, significant to maintainability in high-demand conditions. In this case, the thickness and geometry of the specimen greatly influence the resulting fracture toughness values. Thick specimens have been found to exhibit different fracture behavior than thin specimens due to differences in the crack-tip stress fields, stress triaxiality, and constraint. This is due to the fact that as long as the thickness is sufficiently small, the stress in the region of the fracture conditions are a function of specimen thickness (B). Estimation of the stress intensity factor is very stable when the thickness is above the critical size. This theoretical stress intensity factor is referred to as the plane-strain fracture toughness (K_{Ic}). Hence, knowledge of thickness influence is crucial to reliable hybrid AMC fracture behaviour predictions for their safe use in engineering applications. According to ASTM E-399 testing guidelines, Ramesh et al. [8] and Hareesha et al. [6] also investigated the FT of Al-SiCp composites at an crack length to width (a/W) ratio of 0.45. The impact of increasing the weight percentage of SiCp reinforcement on tensile strength and fracture toughness was assessed by Prasad et al. [9].

Fracture toughness experiments were carried out by Kulkarni D M et al. [10] in order to produce data regarding the fracture behaviour of extra deep drawn (EDD) (0.06%C) steel sheets. "Load-drop" is the fracture criterion applied to the same CT specimens. As specimen thickness increased, it seemed that the fundamental crack tip opening displacement (CTOD) was increasing and approaching a higher limitation value. Yi-Lan Kang et al. conducted an experimental study on copper foils with thicknesses (t) ranging from 0.02 to 1 mm [11]. The study aimed to explore how thickness influences the fracture toughness of metallic foils. Double-edged fractured specimens were used in the experiment to achieve this. According to the experimental results, the specimen's fracture toughness rises with specimen thickness, peaks at about 0.3 mm, and then falls with increasing thickness. In order to evaluate the fracture toughness of materials in the transition temperature range, Toshiyuki Meshii et al. performed studies on CT specimens, as described in [12]. The study also delved into the influence of specimen thickness on 0.55% carbon steel S55C. The research anticipated that T33-stress would affect the crack-tip triaxiality and subsequently influence the out-of-plane behaviour. Marco Palombo et al. [13] attempted to establish the correlation criteria between specimen thickness, CTOD, and fracture toughness. They conducted CTOD tests on a carbon steel material using various sized SENB specimens to accomplish the same. They established the correlation through the experiment data which allowed for the assessment of fracture toughness and CTOD for specimens of varying thicknesses from the specimens that were tested.

The ASTM E399 standard CT specimens with various thicknesses were tested to determine the fracture toughness of Al6061-SiC-cenosphere composites by looking at the thickness of the specimen as one of the factors in a range of fracture

toughness. Raviraj et al. [14] studied the fracture behavior of the Al6061-TiC particle composite. Compact tension (CT) test specimens with varying thickness to width (B/W) ratios between 0.2-0.7 and having an a/W ratio of 0.5 were used. The article presented the load vs. crack tip opening displacement (CTOD) data to compute the fracture toughness on the basis of varying specimen thicknesses. The comparisons of the numerical stress intensity factor are made by three-dimensional (3D) finite element (FE) simulations and experiments. FE simulations are executed to simulate the fracture conditions and give information on the stress and strain field at the crack tip that supplements the understanding of the fracture behavior of the material. The scanning electron microscope (SEM) is also utilized in the analysis of the fracture surfaces that provides data on the micro-mechanisms governing crack growth and failure in the composite material.

The research issue of this study is identification of the relationship between the thickness of the specimen and fracture toughness of Al6061-SiC-cenosphere hybrid composites. Prediction of fracture behavior for hybrid composites at any thickness accurately is the largest drawback, which is an important part of safe part design. The novelty in this research is in the blending of numerical and experimental methods, which also enables a coupled evaluation of the effect of thickness variations on fracture toughness while simultaneously addressing the problem in the literature that has limited data associated with thickness-dependent fracture behavior in hybrid AMCs.

The work investigates the fracture toughness of composite material Al6061-SiC-Cenosphere using the tool of CT (compact tension) specimens manufactured in various thickness levels based on ASTM E399 standards. Fracture toughness of composite blends is analyzed by conducting experiments on the samples. Experiments are accompanied by finite element analysis based on commercial finite element packages. Then, SIF is determined and validated with experiments for a complete evaluation. In addition, the use of a scanning electron microscope (SEM) for the examination of fracture surfaces allows the study to identify the micro-mechanisms responsible for the formation of the fractures and to provide an understanding of the material's failure mode.

MATERIALS AND PROCESSING

One of the key benefits of particulate-reinforced metal matrix composites (MMCs) is their property of being almost isotropic throughout the material [15]. The usual materials used for reinforcing aluminum matrices are silicon carbide (SiC), boron carbide (B_4C), aluminum oxide (Al_2O_3), and graphite. On the other hand, cenosphere particles open up a whole new avenue for the improvement of mechanical and fracture properties of aluminum composites because of their low density which makes them suitable for aerospace and automotive applications where mass reduction is a critical factor. Cenosphere reinforcement, while reducing the composite's density, can at the same time lower its strength when applied in high proportions.

Nevertheless, the hybrid aluminum MMCs which have cenosphere together with SiC reinforcement, for instance, can deliver both strong and lightweight properties. Hybrid AMCs have great potential for research purposes as they might, for example, enhance fracture behaviour to avoid cracking. Earlier investigations indicate that the presence of high SiC in aluminum does not always lead to increased hardness and the fact that SiC (3.22 g/cc) has a much higher density than aluminum (2.65 g/cc) makes low SiC weight fractions a better option for obtaining properties such as hardness increase and weight reduction [15]. In the present study, 3 wt% SiC content is selected based on the literature which associates this amount with the simultaneous improvement of hardness and strength and the retention of low density.

The addition of cenosphere reinforcement results in a further reduction of the composite density which is advantageous for weight-sensitive applications like automotive manufacturing [16]. However, the cenosphere content does not only increase hardness and strength up to about 8 wt% but also causes a decrease in strength beyond this limit. Therefore, the current research investigates the 3, 6, and 9 wt% cenosphere contents. Composite properties are improved due to high silicon oxide content in cenospheres [17], and their Young's modulus of 61.81 GPa means they have stiffness and elasticity that aid in reducing deformation. Thus, these traits render cenosphere as an indispensable material for reinforcement in composites, construction, and insulation among others.

The stir casting method was applied to prepare the composite samples by melting aluminum in a furnace and adding the preheated SiC (3 wt%) and cenosphere (3, 6, and 9 wt%) particles. A pre-heating process of 350 °C for 60 min was done for the SiC and cenosphere powders to remove any moisture and oils that might have been adsorbed before adding them to the melt. A cover flux (4% NaCl+45% KCl+10% NaF) was added to the molten metal prior to pouring it into the mold to avoid gas absorption and limit oxidation during casting [18]. The molten Al6061 bath was held at 740–760 °C during additions; the melt was held for 5–10 min after stirring to homogenize. Mechanical stirring at ~500 rpm for 8–12 min was used to disperse particles and minimize agglomeration. The molten composite was then poured into a preheated graphite die for solidification, completing the casting process.

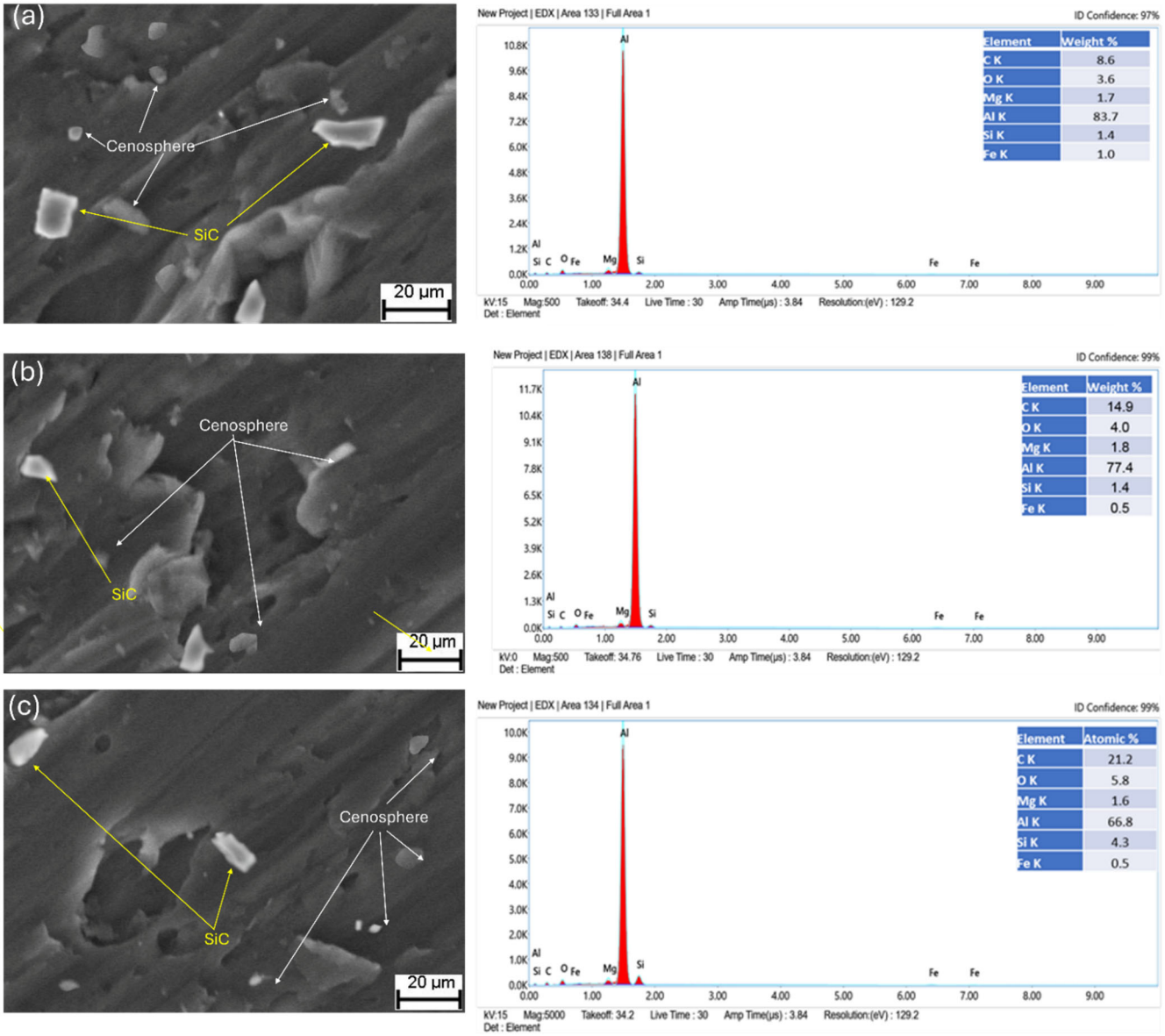

Figure 1: SEM micrographs and corresponding EDS spectra of Al6061–3 wt% SiC composites with different cenosphere contents: (a) 3 wt%, (b) 6 wt%, and (c) 9 wt%.

The energy-dispersive x-ray spectroscopy (EDS) spectra verify the elemental makeup of the reinforcements and the matrix, while the micrographs illustrate the dispersion of SiC and cenospheres within the Al6061 matrix. Both SiC and cenosphere particles are comparatively evenly distributed throughout the matrix at 3 wt% and 6 wt% cenosphere addition (Fig. 1(a-b)), with little clustering. Good wettability throughout the stir casting process is suggested by the unbroken appearance of the reinforcement-matrix interface. The presence of Al, Si, O, and Mg peaks is confirmed by the EDS spectra, with Al predominating because of the matrix. The inclusion of SiC and cenospheres in the composite is confirmed by the Si and O signals. The reinforcing distribution becomes non-uniform at 9 wt% cenosphere loading (Fig. 1c), with notable clumping and indications of weak interfacial bonding in certain areas. The largest percentage of Si and O is confirmed by the EDS analysis, which is in line with the highest reinforcement content. However, there are visible particle agglomerates and porosity, which can reduce the effectiveness of load transfer and negatively impact mechanical qualities. Overall, the SEM–EDS investigations show that higher loading (9 wt%) causes agglomeration and interfacial flaws, whereas lower reinforcement levels (3–6 wt%) encourage better dispersion and stronger interfacial bonding.

EXPERIMENTATION

Test specimen

MMC fracture toughness tests constitute resistance of material and failure to crack propagation under varied loading conditions. In this case, aluminum alloy Al6061 SiC particle-reinforced composite in varying percentage (weight %) are considered for fracture behaviour studies. In line with the provided ASTM E399 requirements, CT specimens preparation was conducted with attention in order to facilitate effective observation of fracture toughness regarding the Aluminum matrix hybrid composites. Fig. 2 provides the CT specimens dimensions in accordance with ASTM standard E399. The CT specimens also meet the given geometric and dimensional requirements of the ASTM standard, e.g., crack length, thickness of the specimen, and notch radius. The CT specimens were accurately machined using CNC wire EDM methods from rectangular blocks of diverse SiC and Cenosphere-strengthened Al6061 MMCs, according to guidelines provided in ASTM Standard E399. The CT specimens were machined into the geometry as indicated in Fig. 2. The CT specimens were machined with diverse thickness to width (B/W) ratios of 0.2, 0.3, 0.4, 0.5, 0.6, and 0.7, as illustrated in Fig. 2.

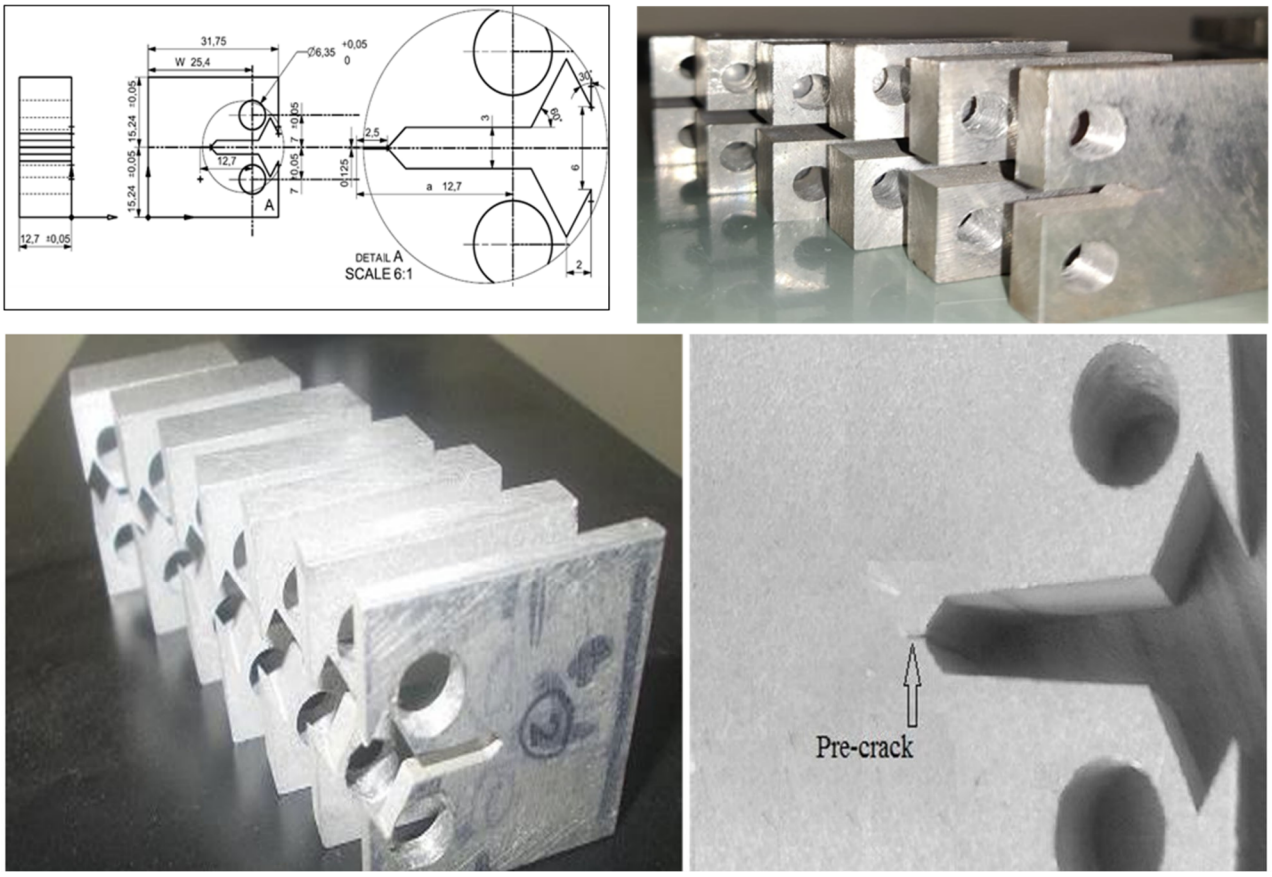

Figure 2: Compact tension specimen and its geometry.

These notches were meticulously prepared to facilitate the controlled introduction of fatigue cracks with specific lengths. These crack lengths were precisely set at 0.7 mm, aligning with predetermined a/W ratios 0.5 [19]. The fatigue cracks were introduced using a servo-hydraulic fatigue testing machine, ensuring a controlled and consistent application of loading conditions, as shown in Fig. 3.

Fracture toughness testing

Fracture toughness was conditioned in a servo-hydraulic testing machine under controlled conditions such that accurate and reliable loading conditions. Fracture toughness was conditioned on compact tension (CT) specimens according to the ASTM E399 standard. The test was conducted in two different phases: fatigue precracking and monotonic fracture testing.

The specimens were precracked under cyclically loading conditions to create a sharp fatigue crack. The load ratio (R) of 0.1 and cyclic frequency of 5 Hz were used to achieve stable crack extension under controlled condition. The precrack length was kept in the designated range of $0.45 \leq a/W \leq 0.55$, and compliance checks were performed to achieve uniformity of the crack front. The CT specimen was constructed with the width (W) of 25.4 mm and thickness (B) of 12.7 mm. A V-notch with initial machined crack length (a_0) of 12 mm was started, and a second fatigue precrack extension of 0.7 mm was started in a servo-hydraulic fatigue precracking machine. Automatic precracking was halted once the accumulation of the crack length was $a \approx 12.7$ mm, thereby obtaining an a/W ratio of approximately 0.5, according to ASTM E399 specifications. After precracking, the specimens were monotonically loaded under displacement control at a constant crosshead speed of 1 mm/min. Displacement control rate permitted one to load slowly and precisely, and it was able to repeat and reproduce test conditions. Load and crack mouth opening displacement (P–CMOD) were collected continuously. The critical load (P_Q) was calculated using the ASTM E399 algorithm, and the corresponding conditional fracture toughness (K_Q) was calculated.

Figure 3: CT specimen in experimental setup.

During the process of fracture toughness testing, the CT specimen is gripped firmly in the fixture wedged between the lower and the upper jaw of the servo-hydraulic testing machine. A clip gauge is mounted on the notch area of the CT specimen. Under loading by the testing machine, the specimen's behavior is closely monitored. In the test, crack mouth opening displacement (CMOD) and the applied load are closely monitored and measured. Measurement can be done with interfaces between a computer and the testing machine. Interfaces facilitate the acquisition of real-time data with the consequence of acquiring precise measurements of load and displacement and recording them digitally.

Throughout the experimental process, the critical load (P_Q) and corresponding CMOD are closely watched for each and every CT specimen. The initial fracture toughness (K_Q) can be determined from the monitored P_Q value through use of available empirical relations. But in order for K_Q to be calculated to be eligible as the true fracture toughness (K_{Ic}), precise CT specimen geometry requirements have to be met, namely on the crack length (a), width (W), and thickness (B) of the specimen.

Satisfaction of requirements related to plain strain fracture toughness is of paramount importance [15]. If the geometric requirements are consistent with the requirements, as stipulated in ASTM [7,20], the provisional fracture toughness (KQ) obtained by calculation can be used as a reliable estimate of the actual fracture toughness (K_{Ic}) [21]. This evaluation will ensure that the fracture toughness formulated effectively captures the ability of the material to arrest crack growth under certain loading conditions.

3D modeling and FE analysis

Fracture toughness was determined through finite element analysis (FEA) using commercially available FE packages, with a focus on static structural analysis for fracture mechanics. This method calculates fracture parameters, such as stress intensity factors (K_I, K_{II}, K_{III}) and energy release rates (G_1, G_2, G_3, G_{Total}), which help predict crack stability and potential failure. The mode one stress intensity, K_I, indicates crack opening under tension and is compared with K_{Ic} to assess the likelihood of crack propagation. Material properties, including hardness and tensile strength of Al6061-SiC/Cenosphere

composites from experimental data, were applied using the materials library. Fig. 4 illustrates the part modeling of the compact tension (CT) sample, conforming to the ASTM standard, which was created using Solid edge and subsequently imported into ANSYS for further analysis. Fig. 4 shows the three-dimensional (3D) models of CT specimens corresponding to different B/W ratios at a/W = 0.5.

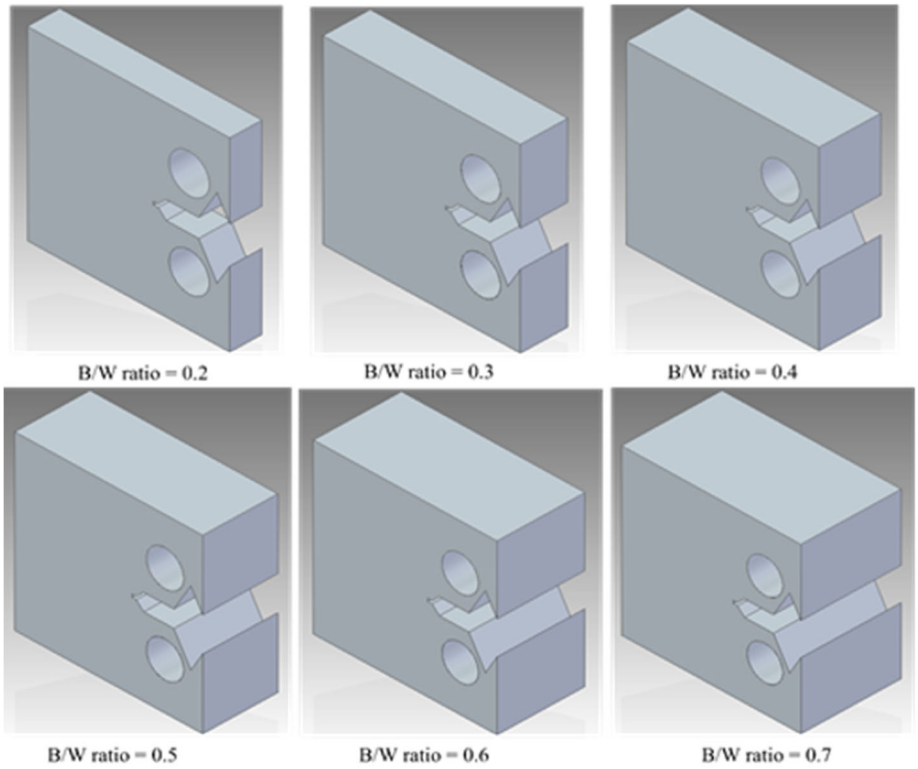

Figure 4: 3D model of CT specimens for different B/W ratios.

Fig. 5 visually illustrates the CT specimen integrated with pre-crack meshing. The introduced crack is a semi-elliptical shape [3,22,23], which is having curved crack front [14], as it is meant to simulate the crack introduced in the fatigue testing machine. Experimentally, fatigue pre-cracks in CT specimens often show a semi-elliptical surface profile, particularly at early stages. To reflect the actual specimen, the crack was modeled as semi-elliptical, and mesh convergence checks were performed to ensure accurate SIF distribution. This meshing technique involves discretizing the specimen's geometry into smaller elements, allowing for accurate simulation of crack propagation behaviour. By applying pre-crack meshing, the computational model can effectively capture the stress distribution and crack propagation pathways within the CT specimen. The bond between the top and bottom halves of the specimen was broken deliberately in order to obtain the crack. The broken face is half, and the symmetrical half is put on the other half. The fatigue pre-crack geometry, as depicted in Fig. 5, is outlined in the test reports [24]. The CT specimen was modeled and meshed using SOLID185 elements in ANSYS, which are 8-node quadratic tetrahedral elements capable of accurately capturing stress singularities near the crack front. A semi-elliptical surface crack was introduced, and a singular quarter-point formulation was applied along the crack front to ensure accurate stress intensity factor (SIF) evaluation, shown in Fig. 5. The semi-elliptical crack [3,19] was defined within the model with nodes strategically positioned along the crack front line. A mesh convergence study was performed to evaluate the effect of mesh size on the calculated fracture toughness K_{Ic}. As the mesh was refined from 1.2×10^{-4} m to 0.6×10^{-4} m, K_{Ic} decreased from 23.3 to 21.44 MPa$\sqrt{m}$. Beyond 0.6×10^{-4} m, the values stabilized (≈21.44–21.45), indicating convergence. Therefore, a mesh size of 1×10^{-4} m was selected to model the crack accurately.

After creating meshing of 3D model, the next step involved incorporating boundary conditions to the components. The inner surface of the portion with holes was subject to displacement control, which is evidenced in Fig. 6. According to the ASTM E399 [7] standard, the CT specimen sits between two jaws, one (lower) fixed jaw and the other to move to be utilized when applying the load. The necessary load (at point B) for simulation was extracted from the experiment [25].

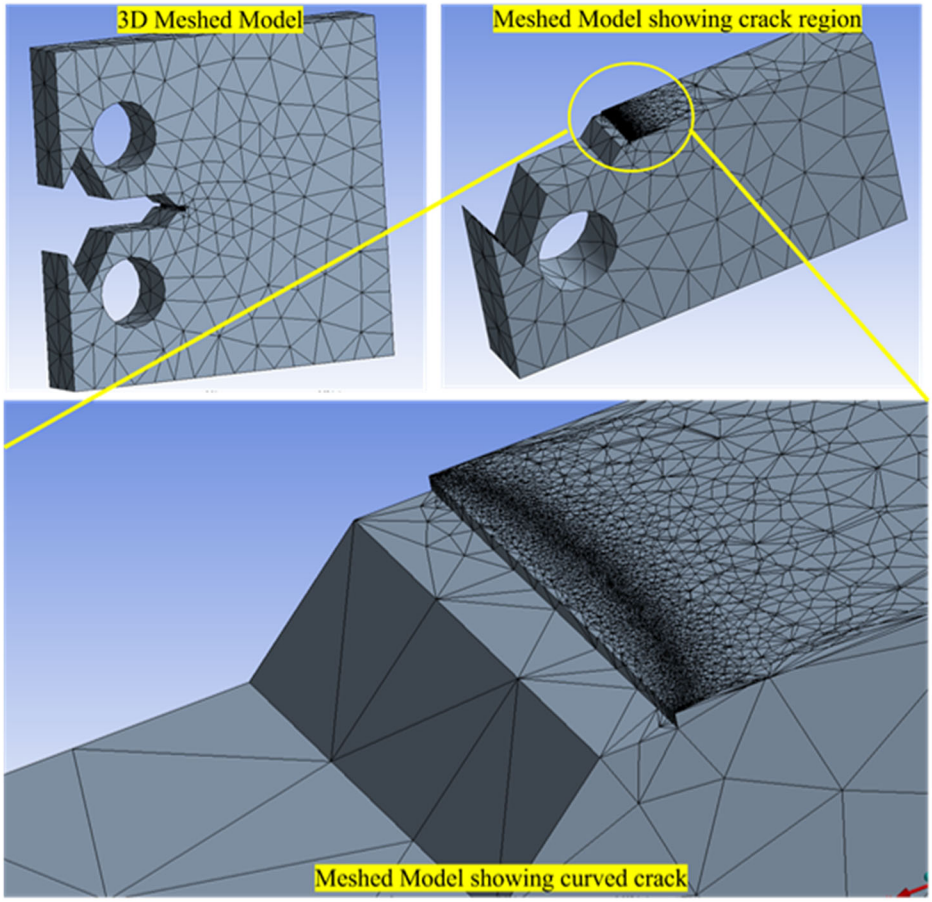

Figure 5: CT Specimen with pre-crack meshing.

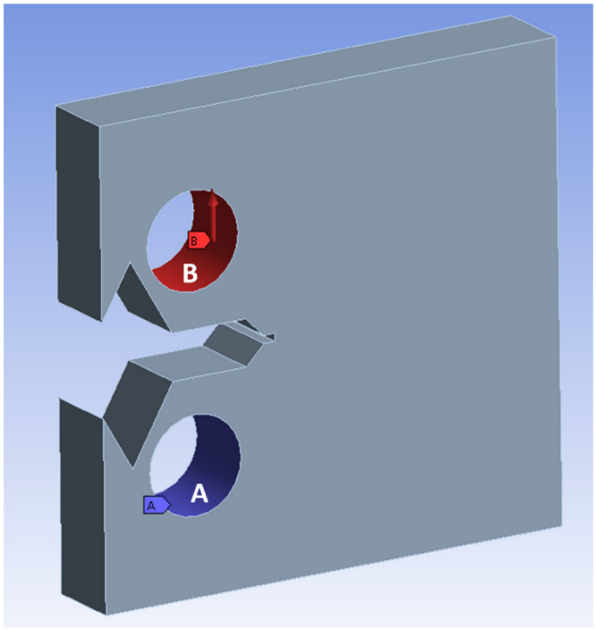

Figure 6: Loading and boundary conditions Tensile load (B) with fixed displacement (A).

The essential outcomes, including von-Mises stress, CTOD (crack tip opening displacement), Mode-1 SIF, deformation, force reactions, and more, can be incorporated into the solution phase. Subsequently, the database file should be resolved

utilizing a finite element solver, concluding the preparatory stages of the finite element analysis (FEA) for the Al6061-3%SiC-3-9wt% cenosphere composite.

RESULTS AND DISCUSSIONS

Experimental results

In this investigation, specimen thickness is systematically varied while keeping other parameters constant, enabling an examination of how fracture toughness is impacted by alterations in thickness. Precious data concerning structural integrity alterations and resistance to crack growth for various material thickness levels are given by this calculation, being an integral component of regular engineering discipline and structural design considerations. The critical SIF (K_I) calculated is plotted graphically versus absolute thickness to width (B/W) ratios for various configurations of Al6061-SiC-cenosphere hybrid composite as shown in Fig. 7(a-c).

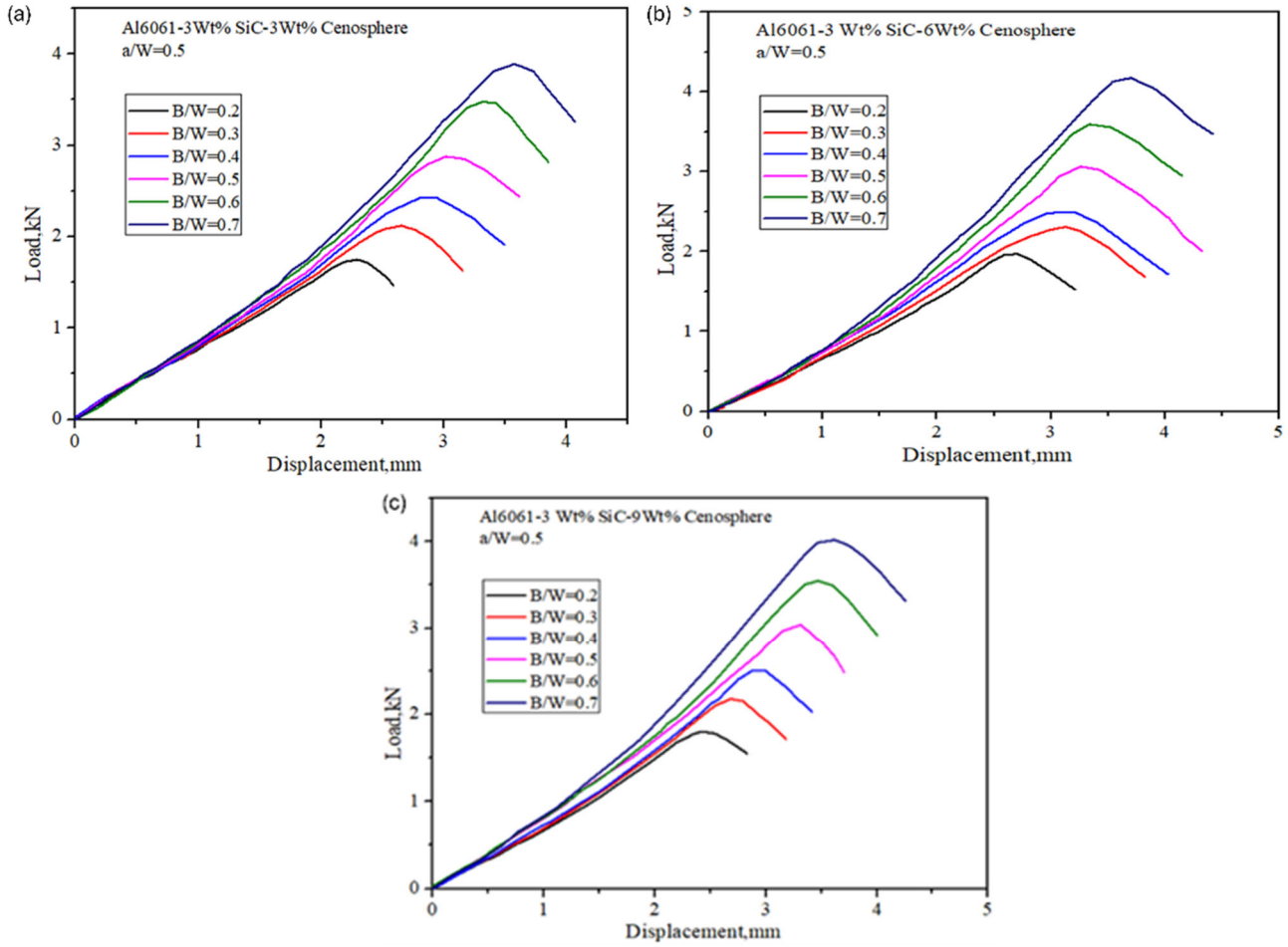

Figure 7: Load vs. CMOD curves for Al6061+3wt%SiC composite of various B/W ratios (a) 3wt% (b) 6wt% (c) 9wt% Cenosphere.

Additionally, Fig. 8 illustrates the trend of K_Q value variation under plane stress condition (K_Q) with varying B/W ratio for Al6061-SiC-cenosphere hybrid composite material. The trend of variation of K_Q value with varying B/W ratio observed is that K_Q value decreases and reaches a constant value at B/W ratios ≥ 0.5. This trend may be philosophically justified in terms of the role of test specimen geometry on stress distribution near the crack tip.

With an increase in the B/W ratio, specimen thickness becomes a more dominant issue in stress distribution and consequently influences the value of K_Q. With values of B/W ≥ 0.5, specimen thickness becomes a critical issue in stress distribution, hence providing a standard value of K_Q. This follows the concept of plane strain fracture toughness (KIc), where the material will experience negligible lateral deformation with its thickness effects.

The rise of fracture toughness from 14.5 to 15.56 MPa√m as indicated in Fig. 8, is due to the synergistic effect of cenosphere content and SiC reinforcement of Al6061 matrix composites. Cenosphere serves to reduce stress concentration sites and enhance microstructural alignment with a subsequent rise in energy absorption at fracture. SiC reinforcement enhances these features even more, and hence there is initiation of crack as well as slowing down in propagation. These two-way activities reduce stress concentration and enhance interfaces, finally leading to a fracture toughness gain. Particularly, Al-3 wt% SiC-6wt% cenosphere composite enhanced fracture toughness significantly.

The graphical chart in Fig. 9 gives a comparison of the variation of fracture toughness (K_{Ic}) with thickness to width ratio (B/W) for various compositions of Al6061+Silicon+Cenosphere hybrid composite, taking various combinations of a/W and B/W ratios into account. The numerical values 33, 36, and 39 represent composition(s) of the reinforcement composite. In this, the first digit "3" is used to indicate the presence of SiC (Silicon Carbide) and the second digit "3," "6," or "9" is used to indicate the various weight percentages of cenosphere reinforcement (3wt%, 6wt%, and 9wt% respectively). These labels are used to identify and distinguish uniquely the unique compositions of the composite samples that were tested for the fracture toughness, in order to classify the experimental data based on the differences in the reinforcement materials and percentages.

The graph's (Fig. 9) trend is evident with an increase in the *B/W* ratio, the fracture toughness progressively diminishes, eventually stabilizing at a constant value. This stable value signifies the realm of "plain strain fracture toughness," where the resistance to fracture of the material remains consistent despite further changes in the specimen's thickness. Notably, when the *B/W* ratio reaches 0.5 or when the sample's thickness exceeds 12.7mm, the material reliably exhibits plain strain fracture toughness characteristics.

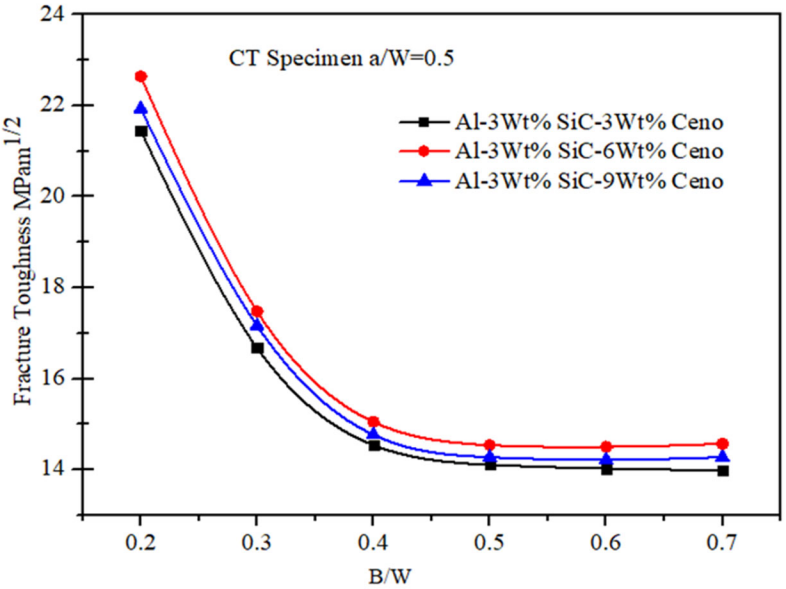

Figure 8: Variation of Critical SIF vs. B/W for various Al6061-SiC cenosphere hybrid composites.

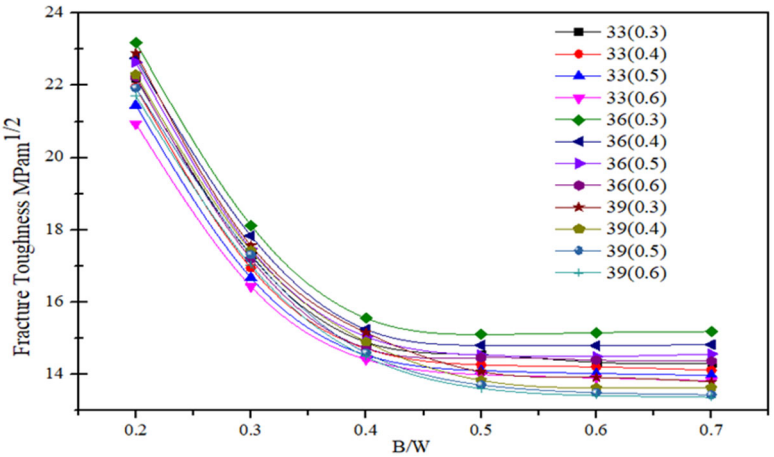

Figure 9: Fracture Toughness v/s B/W graphs for different compositions.

The yield stress (σ_y) and modulus of elasticity (E) for each composite, listed in Tab. 1, were used to verify the plane-strain validity of the measured fracture toughness. Conditional fracture toughness (K_Q) values were determined for various a/W ratios. According to ASTM E399, plane-strain conditions are satisfied when B, a, and (W−a) ≥ 2.5 $(K_Q/\sigma_y)^2$. Tab. 2 compares the required dimensions with actual specimen sizes (B = 12.7 mm, W = 25.4 mm), confirming that all specimens meet the criteria; thus, the measured K_Q values represent valid plane-strain fracture toughness (K_{Ic}).

Sl.No	Composite	Yield stress MPa	Modulus of Elasticity GPa	K_Q, MPa√m a/W=0.5, B/W ratio					
				0.2	0.3	0.4	0.5	0.6	0.7
1	Al6061+3wt%SiC+ 3wt%Cenosphere	247.5±0.59	67.3±1.53	21.45	16.68	14.54	14.11	14.2	14.16
2	Al6061+3wt%SiC+ 6wt%Cenosphere	261±3.57	68.8±0.58	22.64	17.48	15.05	14.54	14.5	14.57
3	Al6061+3wt%SiC+ 9wt%Cenosphere	258±2.15	66.0±3.61	21.93	17.32	14.6	14.3	14.1	13.97

Table 1: Measured yield strength (σ_y), modulus of elasticity (E), at various a/W ratios for Al6061–SiC–Cenosphere hybrid composites.

Sl.No	Composite	ASTM E399 Prerequisite			Actual Specimen size		
		a mm	B mm	W mm	a mm	B mm	W mm
1	Al6061+3wt%SiC+ 3wt%Cenosphere	8.125	8.125	16.251	12.7	12.7	25.4
2	Al6061+3wt%SiC+ 6wt%Cenosphere	7.759	7.759	15.517	12.7	12.7	25.4
3	Al6061+3wt%SiC+ 9wt%Cenosphere	7.680	7.680	15.360	12.7	12.7	25.4

Table 2: Verification of ASTM E399 plane-strain validity for Al6061–SiC–Cenosphere hybrid composites.

FE results

Post-simulation, critical results like SIF, von Mises stress, CTOD, etc., are extracted from the finite element (FE) model. This step emulates the behaviour of the Al6061-SiC-cenosphere composite, enabling comprehensive virtual analysis.

The SIF is used in fracture mechanics to measure the concentration of stress at a fracture tip. In the context of safety design, the fracture susceptibility of a structure or component is assessed by comparing it to a critical threshold that changes according to the characteristics of the material. To examine plasticity levels, simulations were conducted in both linear and non-linear modes using Ansys Workbench, adjusting material properties as needed. The SIF value for the linear simulation was directly obtained from Ansys.

Fig. 10 illustrates the SIF values for the Al6061-3%SiC-3%Cenosphere composite with a/W = 0.5 and B/W = 0.2. The fracture toughness value of 20.08 MPa√m was obtained through finite element simulation. This value represents the material's ability to withstand crack propagation and failure. In parallel, experimental testing yielded a critical load (P_Q) of 3.2 kN, which signifies the load at which crack propagation initiates. By combining the results, for same combination, the calculated fracture toughness value of 21.45 MPa√m showcases resistance against crack propagation of the material and underscores its fracture toughness performance under specific loading conditions.

Since the fracture toughness (K_{Ic}) value remains constant and low as specimen thickness increases, the term "plane strain fracture toughness" describes the material's resistance to crack propagation [3]. The material constant K_{Ic} quantifies a material's ability to withstand crack growth. The plain strain condition, where the plane strain fracture toughness is most noticeable, is met by a specimen thickness of 12.7 mm in this investigation. A conditional fracture toughness value that is consistent with the plane strain fracture toughness was obtained from the ANSYS study. The Al6061-3%SiC-3%cenosphere composite's von-mises stress and plastic zone shape are depicted in Fig. 11, providing information on the plane strain fracture toughness.

The stress distribution under plain strain is fairly comparable to the von-Mises stress distribution often found in metallic materials, as illustrated in Fig. 11, which displays the stress distribution at the fracture tip of the Al6061-3%SiC-3%cenosphere composite. These results validate the conducted simulations. "plane strain fracture toughness" describes fracture toughness in specific situations. The plane strain fracture toughness requirements are met using the finite element simulation model [21]. All different thicknesses of CT specimens have been simulated, and using ANSYS post processor, the magnitudes of K for all composites have been retrieved.

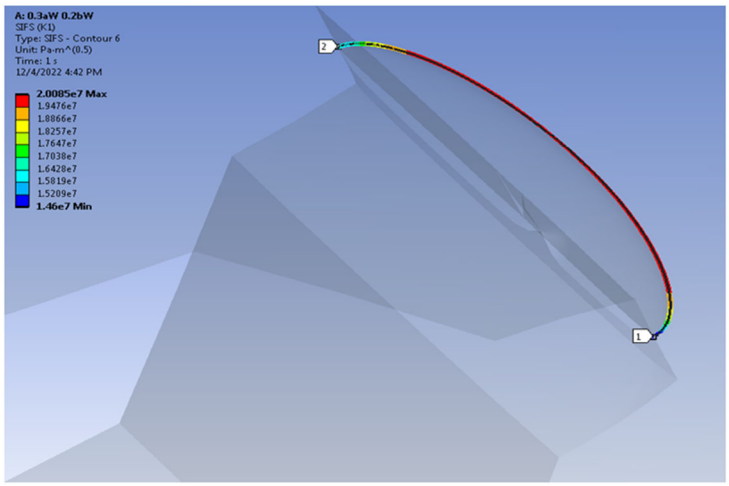

Figure 10: SIF value for Al6061-3%SiC-3%cenosphere composite of a/W = 0.5 and B/W=0.2.

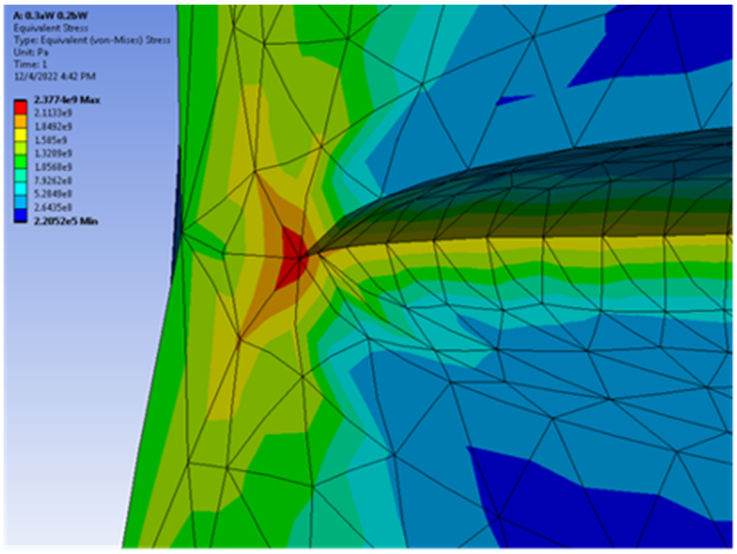

Figure 11: The plane strain state is depicted by the von-Mises stress surrounding the crack point.

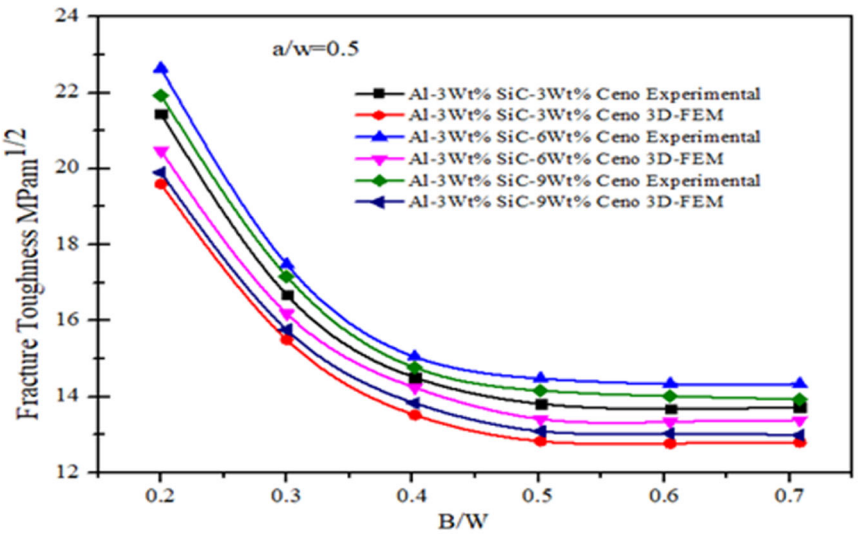

Figure 12: Comparison of the Al6061-SiC-Cenosphere composites' experimental and computational results.

Composite	B/W																	
	0.2			0.3			0.4			0.5			0.6			0.7		
Al6061+3wt%SiC+	Exp	Ansys	% error	Exp	Ansys	% error	Exp	Ansys	% error	Exp	Ansys	% error	Exp	Ansys	% error	Exp	Ansys	% error
3wt%Ceno	21.45	20.0	6.4	16.68	14.97	10.3	14.54	13.2	9.2	14.11	12.6	10.7	14.2	12.8	9.9	14.16	12.7	10.3
6wt%Ceno	22.64	20.5	9.5	17.48	15.8	9.6	15.05	13.9	7.6	14.54	14.2	2.3	14.5	13.5	6.9	14.57	13.5	7.3
9wt%Ceno	21.93	20.3	7.4	17.32	16.1	7.0	14.6	13.6	6.8	14.3	13.1	8.4	14.1	12.76	9.5	13.97	13.5	3.4

Table 3: Comparison of the Al6061-SiC-Cenosphere composites' experimental and computational results for a/W = 0.5.

Tab. 3 compares the experimental and ANSYS-simulated fracture toughness of Al6061–SiC–Cenosphere composites at various B/W ratios. The simulated results closely match the experimental data, with percentage errors generally below 10%. The minor deviations can be attributed to idealized boundary conditions and mesh discretization in the FE model. Overall, the strong correlation between experimental and numerical results validates the accuracy of the finite element simulation approach.

Fractography

The failure mechanism between the matrix (ductile fracture) and particle (brittle fracture, which manifested in bright surfaces) is revealed by the fracture surfaces of the hybrid reinforced composites in Fig. 13. All of the compositions failed because of particle debonding, according to the graphs. However, microcracks have formed in the matrix of the 3wt% Cenosphere composite, and the crack propagation rate is higher since there are fewer particles present. Consequently, it has been noted that fracture toughness has decreased.

Fig. 13(a) depicts the purely ductile fracture for the composite with reduced number of reinforced (6wt %) particles having tiny sized particles. In the aluminium matrix, the SiC and cenosphere particles must function as a barrier to the crack's propagation (Fig. 13(b)). They also cause the fracture route to diverge, allowing the crack to spread around the reinforcing particles and lowering the induced stresses, as seen in Fig. 13(c). The limitation value for fracture propagation is subsequently raised by this barrier caused by SiC and cenosphere particles.

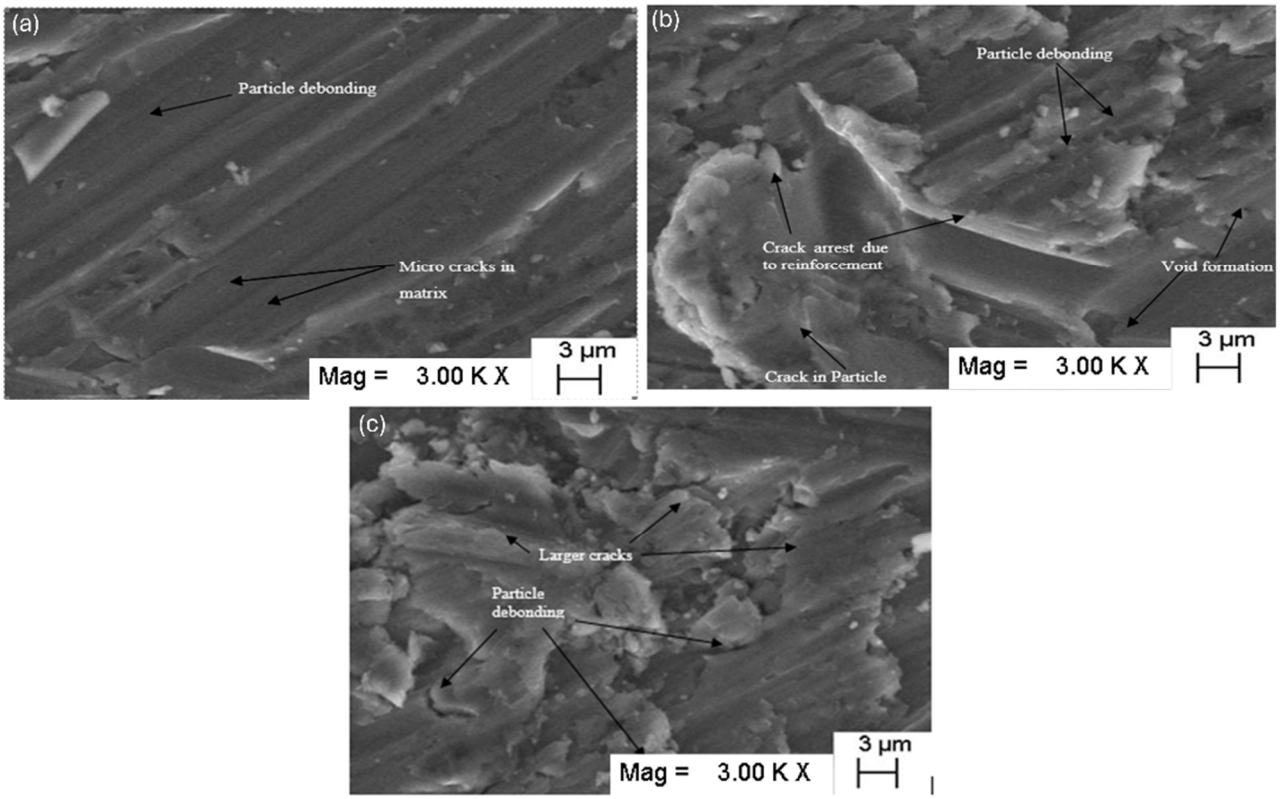

Figure 13: Fractography images of for Al6061+3wt% SiC composites (a) 3wt% (b) 6wt% (c) 9wt% Cenosphere.

Fig. 13(a-b) shows that the matrix cracks propagate early and that the direction of crack propagation changes at particle interaction. As a result, the composite's fracture toughness rises as the crack propagation rate does. However, because large particles are prone to cracking, Fig. 13(c) illustrates the numerous cracks (shown by arrow) that resulted from the increased quantity of large particles, which came from 9wt% of reinforcement.

In the fractography analysis of hybrid reinforced composites (Fig. 13), the fracture surfaces revealed a predominant failure mechanism involving particle debonding. The composite with 3wt% Cenosphere exhibited microcracks in the matrix, leading to increased crack propagation rates and a decrease in fracture toughness. Conversely, the composite with 6wt% particles displayed a ductile fracture with small-sized particles acting as barriers, causing crack path deviation and stress reduction (Fig. 13(b-c)). This barricading effect raised the limiting value of crack growth, thereby increasing fracture toughness. The particle-based cracking interaction also raised greater crack growth rates, which positively affected the fracture toughness of the composite. In the 9wt% composite, however, larger particles caused the development of numerous cracks, which could compromise the integrity of the overall composite structure.

SEM fracture micrographs (Fig. 13) were evaluated using ImageJ, and the average dimple size was 2.65 ± 0.96 μm and the average particle spacing was 0.52 ± 0.22 μm. There are clear signs of particle–matrix debonding and particle fracture on the fractured surface, indicating mixed-mode failure. The evidence of regularly spaced dimples and failed particles indicates good interfacial bonding and effective load transfer from the SiC nanoparticles to Al matrix.

CONCLUSIONS

Fracture toughness of Al6061 alloy composite reinforced with cenosphere particles and SiC was studied employing compact tension (CT) specimens prepared as per ASTM E399 standards. Specimens with different thickness-to-width (B/W) ratios ranging from 0.2 to 0.7 were used to subject controlled fatigue cracks to explore fracture behavior. The effects of specimen thickness on fracture toughness were revealed by finite element simulations and experimental testing; for B/W ratios ≥0.5, the critical SIF (K_Q) stabilised, signifying a shift to plane strain fracture toughness. According to the results, the Al6061-3wt%SiC-6wt% cenosphere composite had the highest fracture toughness (15.56 MPa√m) because of its improved interface strength and efficient stress distribution.

The key conclusions can be summarized as follows:

1. Hybrid composites showed particle debonding as the main failure mechanism. The 3wt% cenosphere composite had reduced fracture toughness due to microcracking, while the 6wt% composite achieved higher toughness due to crack deviation and stress redistribution. However, the 9wt% composite displayed multiple cracking, which could impact integrity.
2. The fracture toughness of Al6061-SiC-cenosphere composites (3wt%–9wt%) ranged from 14.5 to 15.56 MPa√m, depending on cenosphere content.
3. Simulations for each CT specimen thickness, analyzed using a finite element post-processor, aligned well with experimental data, with discrepancies within ±10%, affirming the reliability of the model.

FUNDING

This research received no specific grant from any funding agency in the public, commercial, or not-for-profit sectors.

CONFLICT OF INTEREST

The authors declare that they have no conflict of interest.

REFERENCES

[1] Niyaz Ahamed, M. B., Naveen Kumar, H. S., Anilkumar, S. K., Alqahtani, I., Saleemsab Doddamani, H.G. (2025). Mechanical Properties of SiC Nanoparticle-Reinforced Al-2024 Alloy, Frat. Ed Integrità Strutt., 19(72), pp. 148–61, DOI: https://doi.org/10.3221/IGF-ESIS.72.11.

[2] Doddamani, S., Wang, C., Mohamed, M.J., Arefinkowser, M. (2021). Fracture analysis of aa6061-graphite composite for the application of helicopter rotor blade, Frat. Ed Integrita Strutt., 15(58), pp. 191–201, DOI: https://doi.org/10.3221/IGF-ESIS.58.14.

[3] Bharath, P.B., Shivakumar, S.P., Rajesh, A.M, G. S. Prabhuswamy, S.D. (2025). Effects of specimen thickness and compositions on the fracture toughness investigations of Al7075-SiC/Al2O3 hybrid composites utilizing Taguchi optimization and FEA analysis, Int J Interact Des Manuf, DOI: https://doi.org/10.1007/s12008-025-02269-8.

[4] Alqahtani, I., Niyaz Ahmed, B., Ashoka, E., Rajesh, A. M., Bharath, P. B., & Saleemsab, D. (2025). Indentation Fracture Toughness of Aluminium-Graphite Composites: Influence of Nano-particles, Frat. Ed Integrità Strutt., 19(71), pp. 11–21, DOI: https://doi.org/10.3221/IGF-ESIS.71.02.

[5] Dhummansure, V., Kalyanrao, A.A., Doddamani, S. (2020). Optimization of process parameters for fracture toughness of Al6061-graphite composites, Struct. Integr. Life, 20(1), pp. 51–55.

[6] Guddhur, H., Naganna, C., & Doddamani, S. (2021). Taguchi's method of optimization of fracture toughness parameters of Al-SiCp composite using compact tension specimens, An Int. J. Optim. Control Theor. &Amp; Appl., 11(2), pp. 152–157, DOI: https://doi.org/10.11121/ijocta.01.2021.00990.

[7] ASTM.E399-22. (2022). Standard test method for linear-elastic plane strain fracture toughness KIc of metallic materials, Am. Soc. Test. Mater., , pp. 1–12, DOI: https://doi.org/10.1520/E0399-22.

[8] Ramesh, R S, M V Santhosh Kumar, Y.B., Doddamani, S., K, M.K. (2023). Fracture toughness investigations of AA6061-SiC composites : Effect of corrosion parameters, Mater. Chem. Phys., 308(128224), pp. 1–8, DOI: https://doi.org/10.1016/j.matchemphys.2023.128224.

[9] Prasad, V.S. and R.C. (2004).Tensile and fracture behavior of 6061 al-sicp metal matrix composites. International Symposium of Research Students on Materials Science and Engineering.

[10] Kulkarni, D.M. (2004). The effect of specimen thickness on the experimental and finite element characterization of CTOD in extra deep drawn steel sheets, Sadhana, 29(4), pp. 365–380.

[11] Kang, Y.-L. (2005). Experimental investigations of the effect of thickness on fracture toughness of metallic foils, Mater. Sci. Eng. A, 394, pp. 312–319.

[12] Meshii, T. (2015). Extended investigation of the test specimen thickness (TST) effect on the fracture toughness (Jc) of a material in the ductile-to-brittle transition temperature region as a difference in the crack tip constraint - What is the loss of constraint in the TST, Eng. Fract. Mech., 135, pp. 286–294.

[13] Marco Palombo, Stefano Sandon, M.D.M. (2015). An Evaluation of Size Effect in CTOD-SENB Fracture Toughness Tests, Procedia Eng., 109, pp. 55 – 64.

[14] Raviraj, M.S., Sharanaprabhu, C.M., Mohankumar, G.C. (2016). Experimental investigation of effect of specimen thickness on fracture toughness of Al-TiC composites, Frat. Ed Integrita Strutt., 10(37), pp. 360–368, DOI: https://doi.org/10.3221/IGF-ESIS.37.47.

[15] Saleemsab Doddamani, M.K.K. (2017). Fracture toughness investigations of Al6061-Graphite particulate composite using compact specimens, Frat. Ed Integrità Strutt., 41, pp. 484–490, DOI: https://doi.org/10.3221/IGF-ESIS.41.60.

[16] Vijaya Ramnath B., Elanchezhian C., Jaivignesh M., Rajesh S., Parswajinan C., S.A.G.A. (2014). Evaluation of mechanical properties of aluminium alloy–alumina–boron carbide metal matrix composites, Mater. Des., 58, pp. 332–338.

[17] Sudarshan, M.K.S. (2008). Synthesis of fly ash particle reinforced A356 Al composites and their characterization, Mater. Sci. Eng. A, 480, pp. 117–124., DOI: https://doi.org/10.1016/j.msea.2007.06.068.

[18] Doddamani, S., Kaleemulla, M. (2017). Experimental investigation on fracture toughness of Al6061–graphite by using Circumferential Notched Tensile Specimens, Frat. Ed Integrità Strutt., 11(39), pp. 274–281, DOI: https://doi.org/10.3221/IGF-ESIS.39.25.

[19] Ashoka, E., Sharanaprabhu, C. M. and Krishnaraja, G.K. (2022). Effect of cenosphere and specimen crack lengths on the fracture toughness of Al6061-SiC composites, Frat. Ed Integrità Strutt., 16(61), pp. 473–486, DOI: https://doi.org/10.3221/IGF-ESIS.61.31.

[20] Saleemsab Doddamani, M.K.K. (2019). Effect of Thickness on fracture toughness of Al6061-Graphite, J. Solid Mech., 11(3), pp. 635–43, DOI: https://doi.org/10.22034/jsm.2019.666695.

[21] Kumar, J., Kumar, G., Husain Mehdi, M.K. (2024). Optimization of Process Parameters of Fracture Toughness Using

Simulation Technique Considering Aluminum–Graphite Composites, Int. J. Interact. Des. Manuf., 18(12), pp. 1359–1371, DOI: https://doi.org/10.1007/s12666-020-02113-5.

[22] Jiacai Zhu, Wei Guo, W.G. (2020). Surface fatigue crack growth under variable amplitude loading, Eng. Fract. Mech., 239(107317), DOI: https://doi.org/10.1016/j.engfracmech.2020.107317.

[23] Peng, Z. (2020).Analysis and Numerical Simulation of Fatigue Propagation in Crack Front. 2nd International Conference on Artificial Intelligence and Advanced Manufacture (AIAM), Manchester, United Kingdom, pp. 227–229.

[24] Erke Wang, T.N. and R.R. (1995).A comparison of all-Hexahedra and all Tetrahedral Finite Element Meshes for elastic analysis. Proceedings 4th of international conference, pp. 179–181.

[25] Doddamani, S., Begum, Y., Bharath, K.N., Rajesh, A.M. (2024).Investigation of fracture toughness analysis of polymer composites using finite element analysis. In: Sathish Kumar Palaniappan, Rajeshkumar Lakshminarasimhan, Sanjay Mavinkere Rangappa, S.S., (Ed.), Finite Element Analysis of Polymers and Composites, Woodhead Publishing in Materials, Woodhead Publishing, pp. 149–183.